

April 21, 2022

Violation of the geometric scaling behaviour of the amplitude for running QCD coupling in the saturation region.

Bastian Diaz Saez^a * and Eugene Levin^{a,b} †

^a *Departamento de Física, Centro de Estudios Subatómicos, Universidad Técnica Federico Santa María, and Centro Científico-Tecnológico de Valparaíso, Casilla 110-V, Valparaíso, Chile*

^b *Department of Particle Physics, School of Physics and Astronomy, Tel Aviv University, Tel Aviv, 69978, Israel*

ABSTRACT: In this paper we show that the intuitive guess that the geometric scaling behaviour should be violated in the case of the running QCD coupling, turns out to be correct. The scattering amplitude of the dipole with the size r depends on new dimensional scale: Λ_{QCD} , even at large values $Y = \ln(1/x)$ and $l = \ln(\alpha_S(r^2)/\alpha_S(1/Q_s^2))$. However, in this region we found a new scaling behaviour: the amplitude is a function of $\zeta = Yl$. We state that only in the vicinity of the saturation scale Q_s ($\alpha_S(Q_s^2) \ln(r^2 Q_s^2) \leq 1$), the amplitude shows the geometric scaling behaviour. Based on these finding the geometric scaling behavior that has been seen experimentally, stems from either we have not probed the proton at HERA and the LHC deeply inside the saturation region or that there exists the mechanism of freezing of the QCD coupling constant at $r^2 \approx 1/Q_s^2$.

KEYWORDS: Colour Glass Condensate, gluon saturation, non-linear evolution, geometric scaling behaviour .

PACS: 12.38-t, 12.38.Cy, 12.38.Lg, 13.60.Hd, 24.85.+p, 25.30.Hm

*Email: bastilo_1@hotmail.com

†Email: leving@post.tau.ac.il, eugeniy.levin@usm.cl

Contents

1. Introduction.	1
2. General approach: behaviour of the scattering amplitude in the vicinity of the saturation scale for running QCD coupling	2
3. The non-linear equation with the simplified BFKL kernel for running α_S.	4
3.1 $r^2 \ll 1/Q_s^2$	5
3.2 $r^2 \gg 1/Q_s^2$	5
4. Solutions to the simplified equation	6
4.1 Initial and boundary conditions.	6
4.2 Solution for $\phi \gg 1$	7
4.3 Traveling wave solution	7
4.4 Self-similar solution	8
4.5 Numerical solution	9
5. Conclusions	9

1. Introduction.

The geometric scaling behaviour of the scattering amplitude gives an example of the prediction that based on the most fundamental features of the high parton density QCD. It means that the scattering amplitude of the dipole in the saturation region is a function of one dimensionless variable $\tau = r^2 Q_s^2(Y; b)$ instead of being a function of dipole size (r), energy ($Y = \ln(1/x)$) and impact parameter (b). $Q_s(x, b)$ is the new dimensional scale (saturation momentum) which absorbed entire dependence on energy and impact parameter of the amplitude. The existence of this scale and its appearance from the non-linear evolution at low x is the most fundamental theoretical result of both the BFKL Pomeron calculus [1–5] and the Colour Glass Condensate (CGC) approach [6–9]. The idea of the geometric scaling behaviour is very simple: τ is the only dimensionless variable in the dense system of partons. At the moment we have a general proof of the geometric scaling behaviour of the amplitude in the saturation region [10], two examples of the

analytically solved non-linear Balitsky-Kovchegov equation with simplified kernels [11, 12] which show the geometric scaling behaviour and the proof that this behaviour is a general property of the linear dynamics in the vicinity of the saturation scale [13].

However, analyzing these arguments and proofs one can see that they are related to the case of fixed QCD coupling constant as far as the behaviour of the amplitude in the saturation domain is concerned. Indeed, for frozen QCD coupling we do not have other dimensional parameters but Q_s . For running QCD coupling the situation is not so clear since it brings the second dimensional scale: Λ_{QCD} , and the role of this scale has to be studied in the saturation region.

The paper presents such study in the case of the simplified BFKL kernel (see Ref. [11]). We show that the geometric scaling behaviour is violated for the running QCD coupling and the amplitude does not depend on the one variable τ . It turns out that the amplitude depends on a different variable

$$\zeta = \frac{4N_c}{b} Y \ln \left(\frac{\bar{\alpha}_S(r^2 \Lambda_{QCD}^2)}{\bar{\alpha}_S(\Lambda_{QCD}^2/Q_s^2)} \right) \quad \text{where} \quad \bar{\alpha}_S(r^2) = \frac{4N_c}{b \ln(1/(r^2 \Lambda_{QCD}^2))} \quad (1.1)$$

with $b = 11N_c/3 - 2N_f/3$ for number of colours N_c and the number of flavours N_f . One can see that ζ depends on both dimensional scales: Q_s and Λ_{QCD} .

2. General approach: behaviour of the scattering amplitude in the vicinity of the saturation scale for running QCD coupling

The nonlinear Balitsky-Kovchegov equation for the scattering amplitude of the dipole with size r has the following form [8, 9]:

$$\begin{aligned} \frac{\partial N(r, Y; b)}{\partial Y} = & \int \frac{d^2 r_1}{2\pi} K(r; r_1, r_2) \times \left\{ N\left(r_1, Y; \vec{b} - \frac{1}{2} \vec{r}_2\right) + N\left(r_2, Y; \vec{b} - \frac{1}{2} \vec{r}_1\right) - N\left(r, Y; \vec{b}\right) \right. \\ & \left. - N\left(r_1, Y; \vec{b} - \frac{1}{2} \vec{r}_2\right) N\left(r_2, Y; \vec{b} - \frac{1}{2} \vec{r}_1\right) \right\} \end{aligned} \quad (2.1)$$

where $Y = \ln(1/x)$ is the rapidity of the incoming dipole; N is the imaginary part of the scattering amplitude and b is the impact parameter of this scattering process and $\vec{r}_2 = \vec{r} - \vec{r}_1$. The BFKL kernel $K(r_1, r_2)$ has the following form

$$K(r; r_1, r_2) = \bar{\alpha}_S(r^2) \left\{ \frac{r^2}{r_1^2 r_2^2} + \frac{1}{r_1^2} \left(\frac{\bar{\alpha}_S(r_1^2)}{\bar{\alpha}_S(r_2^2)} - 1 \right) + \frac{1}{r_2^2} \left(\frac{\bar{\alpha}_S(r_2^2)}{\bar{\alpha}_S(r_1^2)} - 1 \right) \right\} \quad (2.2)$$

This kernel takes into account the running QCD coupling and was derived in Re. [14]. In Eq. (2.1) α_S is the QCD coupling

$$\alpha_S(r^2) = \frac{\alpha_S(R^2)}{1 + \frac{\alpha_S(R^2)}{4\pi b} \ln(R^2/r^2)} = \frac{4\pi}{b \ln(1/(r^2 \Lambda_{QCD}^2))} \quad (2.3)$$

and $\bar{\alpha}_S = N_c \alpha_S / \pi$. R is the arbitrary size (so called the renormalization point) which the physical observables do not depend on.

In the vicinity of the saturation scale where $r^2 \approx r_1^2 \approx r_2^2 \approx 1/Q_s^2$ and we can consider that $\bar{\alpha}_S(r^2) = \bar{\alpha}_S(r_1^2) = \bar{\alpha}_S(r_2^2)$. Indeed, choosing $R = r$ we can see that

$$\alpha_S(r_i^2) = \frac{\alpha_S(r^2)}{1 + \frac{\alpha_S(r^2)}{4\pi b} \ln(r^2/r_i^2)} \xrightarrow{\ln(r^2/r_i^2) \ll \ln(r^2 \Lambda_{QCD})} \alpha_S(r^2) \quad (2.4)$$

In the vicinity of the saturation scale $r^2 \propto 1/Q_s^2$ and condition $|\ln(r_i^2 Q_s^2)| \ll \ln(Q_s^2/\Lambda_{QCD})$ determines the kinematic region which we call vicinity of the saturation scale. Using this simplification the kernel of Eq. (2.1) looks as follows:

$$K(r; r_1, r_2) = \bar{\alpha}_S(r^2) \frac{r^2}{r_1^2 r_2^2} \quad (2.5)$$

The second simplification stems from the observation that for the equation for the saturation scale we do not need to know the precise form of non-linear term [2, 12, 15]. Therefore, to find this equation as well as behaviour of the amplitude in the vicinity of the saturation scale we need to solve the linear BFKL equation, but in the way which will be suitable for the solution of the non-linear equation with a general non-linear term. It is enough to use the semiclassical approximation for the amplitude $N(r, Y; b)$, which has the form

$$N_A(Y, \xi) = e^{S(Y, \xi)} = e^{\omega(Y, \xi) Y + (1 - \gamma(Y, \xi)) \xi + S_0} \quad (2.6)$$

where $\xi = \ln(r^2 Q_s^2(Y = Y_0; b))$. In Eq. (2.6) we are searching for functions $\omega(Y, \xi)$ and $\gamma(Y, \xi)$ which are smooth functions of both arguments in the following sense

$$\omega'_Y(Y, \xi) \ll \omega(Y, \xi); \quad \omega'_\xi(Y, \xi) \ll \omega(Y, \xi); \quad \gamma'_Y(Y, \xi) \ll \gamma(Y, \xi); \quad \gamma'_\xi(Y, \xi) \ll \gamma(Y, \xi); \quad (2.7)$$

The BFKL equation near to the saturation scale looks as follows

$$\frac{\partial N(r, Y; b)}{\partial Y} = \bar{\alpha}_S(r^2) \int \frac{d^2 r_1}{2\pi} K(r; r_1, r_2) \times \left\{ N(r_1, Y; \vec{b}) + N(r_2, Y; \vec{b}) - N(r, Y; \vec{b}) \right\} \quad (2.8)$$

In Eq. (2.8) we assume that we are looking for the solution at $b \gg r_1$ or/and r_2 . Substituting Eq. (2.6) into Eq. (2.8) and taking into account that function $(r^2)^f \equiv \exp(f \xi)$ is the eigenfunction of the BFKL equation, namely,

$$\bar{\alpha}_S(r^2) \int \frac{d^2 r_1}{2\pi} K(r; r_1, r_2) (r_1^2)^f = \bar{\alpha}_S(r^2) \chi(f) (r^2)^f \text{ with } \chi(f) = 2\psi(1) - \psi(f) - \psi(1-f) \\ \text{where } \psi(z) = d \ln \Gamma(z) / dz \quad \text{and} \quad \Gamma(z) \text{ is Euler gamma function} \quad (2.9)$$

we obtain that

$$\omega(Y, \xi) = \bar{\alpha}_S(\xi) \chi(\gamma(Y, \xi)) \quad (2.10)$$

This solution has a form of wave-package and the critical line is the specific trajectory for this wave-package which coincides with the its front line. In other words, it is the trajectory on which the phase

velocity (v_{ph}) for the wave-package is the same as the group velocity (v_{gr}). The equation $v_{gr} = v_{ph}$ has the following form for Eq. (2.10)

$$v_{ph} = \bar{\alpha}_S(r^2) \frac{\chi(\gamma_{cr})}{1 - \gamma_{cr}} = -\bar{\alpha}_S(r^2) \chi'(\gamma_{cr}) = v_{gr} \quad (2.11)$$

with the solution $\gamma_{cr} = 0.37$.

Eq. (2.11) can be translated into the following equation for the critical trajectory

$$\frac{d\xi(Y)}{dY} = v_{ph} = \bar{\alpha}_S(\xi) \frac{\chi(\gamma_{cr})}{1 - \gamma_{cr}} \quad (2.12)$$

with the solution

$$\frac{8N_c}{b} \frac{\chi(\gamma_{cr})}{1 - \gamma_{cr}} Y \equiv \xi_s^2 = \xi^2 - \xi_0^2 \quad (2.13)$$

where $\xi_0 = \ln(Q_s^2(Y = Y_0; b)/\Lambda_{QCD}^2)$ and $\xi_s = \ln(Q_s^2(Y, b)/Q_s^2(Y = Y_0, b))$

For finding the behaviour of the amplitude in the vicinity of the line given by Eq. (2.13) one should expand function $\omega(Y, \xi)$ and $\gamma(Y, \xi)$ and find a deviation from the critical line of Eq. (2.13). Replacing $\xi = \xi_s + \Delta\xi$ where $\Delta\xi = \ln(r^2 Q_s^2(Y, b))$ and considering $\Delta\xi \ll \xi_s$ one obtain

$$\begin{aligned} N(Y, \xi) &\propto \exp \left\{ \left(\frac{\partial \omega(Y, \xi = \xi_s)}{\partial \xi} Y + 1 - \gamma \right) \Delta\xi \right\} \\ &= \exp \left\{ \left(\frac{\chi(\gamma_{cr})}{\xi_s^2} Y + 1 - \gamma_{cr} \right) \Delta\xi \right\} \\ &= \left(r^2 Q_s^2(Y, b) \right)^{\frac{3}{2}(1-\gamma_{cr})} \end{aligned} \quad (2.14)$$

It should be mentioned that everything, except Eq. (2.14), are not new and have been studied in details before (see for example Refs. [2, 12, 15]). We discuss them here for the completeness of presentation. Eq. (2.14) shows that the running QCD coupling leads to a different behaviour of the scattering amplitude in the vicinity of the critical trajectory. Recall that for frozen $\bar{\alpha}_S$ the amplitude $N \propto (r^2 Q_s^2)^{-(1-\gamma_{cr})}$. Concluding this section we would like to stress that we obtain the geometric scaling behaviour of the scattering amplitude to the right of the critical curve ($\tau > 1$) in the case of the running α_S . This result gives us a hope that inside the saturation region we can observe the geometric scaling behaviour as well.

3. The non-linear equation with the simplified BFKL kernel for running α_S .

The solution to the Balitsky-Kovchegov equation with the kernel of Eq. (2.2) has not been found. Following Ref. [11] we simplify the kernel by taking into account only log contributions. In other words, we would like to consider only leading twist contribution to the BFKL kernel, which contains all twists. Actually we have two types of the logarithmic contributions: $\ln(r^2 \Lambda_{QCD}^2)$ for $r^2 \ll 1/Q_s^2$ and $\ln(r^2 Q_s^2)$ for $r^2 > 1/Q_s^2$.

3.1 $r^2 \ll 1/Q_s^2$

In this kinematic region we can simplify $K(r; r_1, r_2)$ in Eq. (2.2) in the following way [11], since $r_1 \gg r$ and $r_2 = |\vec{r} - \vec{r}'| > r$

$$\int d^2 r' K(r, r_1, r_2) \rightarrow \pi \bar{\alpha}_S(r^2) r^2 \int_{r^2}^{\frac{1}{\Lambda_{QCD}^2}} \frac{dr'^2}{r'^4} \quad (3.1)$$

Introducing $\tilde{N}(r, Y; b) = N(r, Y; b) / (\bar{\alpha}_S(r^2) r^2)$ we obtain

$$\frac{\partial \tilde{N}(r, Y; b)}{\partial Y} = \int_{r^2}^{1/\Lambda_{QCD}^2} dr'^2 \left\{ \frac{\bar{\alpha}_S(r'^2)}{r'^2} \tilde{N}(r', Y; b) - \frac{\bar{\alpha}_S^2(r'^2)}{2} \tilde{N}^2(r', Y; b) \right\} \quad (3.2)$$

One can see that the simplified kernel of Eq. (3.1) sums $\left(\int_{r^2}^{1/\Lambda_{QCD}^2} dr'^2 \frac{\bar{\alpha}_S(r'^2)}{r'^2} \right)^n$. As we have discussed in the previous section the form of non-linear corrections is not important here. One can see that the linear part of Eq. (3.2) gives the familiar GLAP equation in the double log approximation [16].

3.2 $r^2 \gg 1/Q_s^2$

The main contribution in this kinematic region originates from the decay of the large size dipole into one small size dipole and one large size dipole. However, the size of the small dipole is still larger than $1/Q_s$. It turns out that $\bar{\alpha}_S$ depends on the size of produced dipole if this size is the smallest one. It follows directly from Eq. (2.2) in the kinematic regions: $r \approx r_2 \gg r_1 \gg 1/Q_s^2$ and $r \approx r_1 \gg r_2 \gg 1/Q_s^2$ (see Ref. [17] for additional arguments). This observation can be translated in the following form of the kernel

$$\int d^2 r' K(r, r') \rightarrow \pi \int_{1/Q_s^2(Y, b)}^{r^2} \frac{\bar{\alpha}_S(r_1^2) dr_1^2}{r_1^2} + \pi \int_{1/Q_s^2(Y, b)}^{r^2} \frac{\bar{\alpha}_S(r_2^2) dr_2^2}{r_2^2} \quad (3.3)$$

One can see that this kernel leads to the $\left(\int_{1/Q_s^2(Y, b)}^{r^2} \frac{\bar{\alpha}_S(r_1^2) dr_1^2}{r_1^2} \right)^n$ -contributions. Introducing a new function

$$\tilde{N}(r, Y; b) = \int_{1/Q_s^2}^{r^2} dr'^2 \frac{\bar{\alpha}_S(r'^2)}{r'^2} N(r', Y; b) \quad (3.4)$$

one obtain the following equation

$$\frac{\partial N(r, Y; b)}{\partial Y} = \tilde{N}(r, Y; b) \left(1 - N(r, Y; b) \right) \quad (3.5)$$

Introducing a new variable

$$l = \int_{r^2}^{r'^2} dr'^2 \frac{\bar{\alpha}_S(r'^2)}{r'^2} = \frac{4N_c}{b} \ln \left(1/\bar{\alpha}_S(r^2) \right) = \frac{4N_c}{b} \ln(\bar{\xi}) \quad (3.6)$$

with $\bar{\xi} = -\ln(r^2 \Lambda_{QCD}^2) \equiv -\xi$ and new function $\phi(r, Y; b)$

$$N(r, Y; b) = 1 - e^{-\phi(r, Y; b)} \quad (3.7)$$

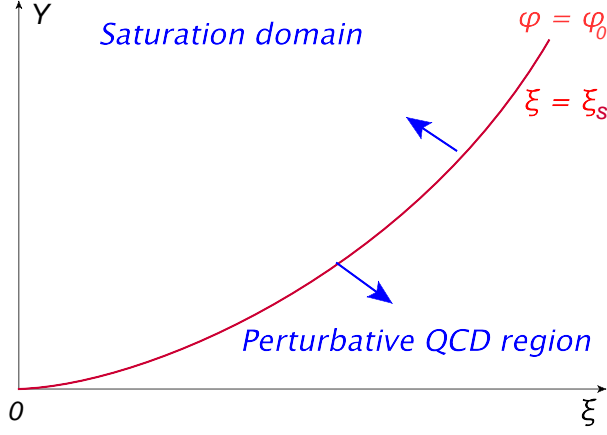


Figure 1: Kinematic regions for the dipole scattering: $\xi = -\ln(r^2 \Lambda_{QCD}^2)$ and $\xi_s = \ln(Q_s^2/\Lambda_{QCD}^2)$. The red line is the critical trajectory with the equation $\frac{32N_c}{b} Y = \xi^2$ (see Eq. (4.3)) on which $\phi(Y, \xi = \xi_s) = \phi_0$.

we obtain the following equation

$$\frac{\partial^2 \phi(r, Y; b)}{\partial Y \partial l} = 1 - e^{-\phi(r, Y; b)} \quad (3.8)$$

4. Solutions to the simplified equation

4.1 Initial and boundary conditions.

The simplified BFKL kernel looks as follows [11] in ω and γ representation (in double Mellin transform with respect to Y and ξ)

$$\chi(\gamma) = \begin{cases} \frac{1}{\gamma} & \text{for } r^2 \leq 1/Q_s^2; \\ \frac{1}{1-\gamma} & \text{for } r^2 > 1/Q_s^2; \end{cases} \quad (4.1)$$

Using this kernel for small values of r^2 ($r^2 < 1/Q_s^2$) and the general formulae of Eq. (2.13) and Eq. (2.14) one can write the initial conditions at $\tau = r^2 Q_s^2 = 1$. They are

$$\phi(Y, \bar{\xi} = \xi_s; b) = \phi_0; \quad \frac{\partial \phi(Y, \bar{\xi} = \xi_s; b)}{\partial \bar{\xi}} = -\frac{3}{4}\phi_0 \quad (4.2)$$

The critical line that gives us the energy dependence of the saturation scale has the form (see Eq. (2.13))

$$\frac{32N_c}{b} Y = \bar{\xi}^2 \quad (4.3)$$

In Eq. (4.3) we assume that $\xi_0 = 0$. It means that we consider the scattering amplitude for the dipoles of all sizes smaller than $r_0 = 1/\Lambda_{QCD}$ and the entire kinematic region can be divided in two parts: the region of perturbative QCD and the saturation domain (see Fig. 1).

4.2 Solution for $\phi \gg 1$

Searching for the solution to Eq. (3.8) we start with finding the asymptotic behaviour of ϕ at large values of Y and l . We expect that ϕ will be large in this region since that dipole amplitude tends to be close to unity due to unitarity constraints. Therefore, in this region Eq. (3.8) degenerates to a very simple equation

$$\frac{\partial^2 \phi(Y, l; b)}{\partial Y \partial l} = 1 \quad (4.4)$$

with obvious solution:

$$\phi_\infty(Y, l; b) = Yl + F(Y) + G(l) \quad (4.5)$$

where functions F and G should be found from the initial conditions of Eq. (4.2).

The final solution has the form

$$\tilde{\phi}_\infty(Y, l; b) = Y(l - l_s) - \frac{3}{4}\phi_0(e^l - e^{l_s}) - \frac{1}{2}(e^{2l} - e^{2l_s}) + \phi_0 \quad (4.6)$$

where $l_s = \frac{N_c}{b} \ln \xi_s$.

Therefore, we learned two lessons in this subsection: (1) the main problem with Eq. (3.8) is to satisfy the initial and boundary conditions; and (2) the asymptotic solution does not show a geometric scaling behaviour since even the simplest solution of Eq. (4.6) does not depend on the variable $z = \xi_s - \bar{\xi}$. However, the solution of Eq. (4.6) at $\bar{\xi} \rightarrow \xi_s$ has the following form

$$\tilde{\phi}_\infty(Y, l; b) \xrightarrow{\bar{\xi} - \xi_s \ll \xi_s} \phi_0 - \frac{3}{4}\phi_0(\bar{\xi} - \xi_s) = \phi + \frac{3}{4}\phi_0 z \quad (4.7)$$

showing the geometric scaling behaviour. Hence, we can hope that the solution will show the geometric scaling behaviour in the vicinity of the saturation scale.

On the other hand, the solution given by Eq. (4.6), leads to $\phi_\infty < 0$ and, therefore, contradicts the unitarity constraints, leading to the negative imaginary part of the amplitude. Such behaviour stems from that terms in Eq. (4.6) which are responsible for the matching of the $\partial\phi/\partial l$ at $l \rightarrow 0$. Hence we have to find a different solution which has the same behaviour $\phi_\infty = Yl$ for $\phi \gg 1$.

4.3 Traveling wave solution

Eq. (3.8) has general traveling wave solution (see Ref. [21] formula **3.5.3**) which can be found noticing that $\phi(Y, l; b) \equiv \phi(\eta \equiv aY + bl; b)$ reduced the equation to

$$ab \frac{d^2 \phi(\eta; b)}{d\eta^2} = 1 - e^{-\phi(\eta; b)} \quad (4.8)$$

The general solution of Eq. (4.8) has the form

$$\int_{\phi_0}^{\phi} \frac{d\phi'}{\sqrt{c + \frac{1}{2ab}(\phi' - 1 + e^{-\phi'})}} = \eta = aY + bl \quad (4.9)$$

where c, ϕ_0, a and b are arbitrary constants that should be found from the initial and boundary conditions.

The initial conditions of Eq. (4.2) can be written in terms of Y and l variables as

$$\phi(\eta = aY + bl_s; b) = \phi_0; \quad \phi'_\eta(\eta = aY + bl_s; b) = -\frac{3}{4}\phi_0\xi_s \quad (4.10)$$

It should be mentioned that the variable η is not the scaling variable $z = \ln(\tau) = \xi_s - \bar{\xi}$ with $\xi_s = \sqrt{\frac{32N_c}{b}Y}$. One can see that we cannot satisfy the initial conditions of Eq. (4.10). Indeed, even to satisfy the first of Eq. (4.10) we need to choose $\eta = 0$ on the critical line. As you see we cannot do this with a and b being constants. The second equation depends on Y , but not on η , making impossible to satisfy this condition in the framework of traveling wave solution.

If we try to find a solution which depends on z ($\phi(Y; r^2; b) = \phi(z; b)$) we obtain the following equation (using the variable $\tilde{z} = \sqrt{\frac{16N_c}{b}}z$)

$$\sqrt{\frac{16N_c}{b}} \frac{\tilde{z}}{\sqrt{2Y}} \frac{d^2\phi(\tilde{z}; b)}{d\tilde{z}^2} + \frac{d^2\phi(\tilde{z}; b)}{d\tilde{z}^2} = 1 - e^{-\phi(\tilde{z}; b)} \quad (4.11)$$

Therefore, only in the vicinity of the critical line where $\sqrt{\frac{16N_c}{b}}\tilde{z} \ll \sqrt{2Y}$ we can expect the geometric scaling behaviour of the scattering amplitude. It should be stressed that at large value of Y the region where we have the geometric scaling behaviour becomes rather large. Neglecting the first term in Eq. (4.11) we obtain the equation in the same form as for frozen α_S . It is easy to find the solution to this equation that satisfies the initial condition of Eq. (4.2). Actually, the condition $\sqrt{\frac{16N_c}{b}}\tilde{z} \ll \sqrt{2Y}$ can be rewritten as $\alpha_S(Q_s^2) \ln(r^2 Q_s^2) \ll 1$ and it shows the region in which we can consider the running QCD coupling as being frozen at $r^2 = 1/Q_s^2$.

4.4 Self-similar solution

Generally speaking (see Ref. [21] formulae **3.4.1.1** and **3.5.2**) Eq. (3.8) has a self similar (functional separable) solution $\phi(Y, l; b) = \phi(\zeta; b)$ with (see also Eq. (1.1))

$$\zeta = Y(l - l_s) \quad (4.12)$$

For function $\phi(\zeta; b)$ we can reduce Eq. (3.8) to the ordinary differential equation

$$(\zeta - 2) \frac{d^2\phi(\zeta; b)}{d\zeta^2} + \frac{d\phi(\zeta; b)}{d\zeta} = 1 - e^{-\phi(\zeta; b)} \quad (4.13)$$

The initial condition of Eq. (4.2) can be rewritten in the form

$$\begin{aligned} \phi(\zeta = 0; b) &= \phi_0; \\ \frac{d\phi(\zeta = 0; b)}{d\zeta} &= -\frac{3}{4}\phi_0/\xi_s = -\frac{3}{4}\phi_0/\sqrt{\frac{32N_c}{b}Y} \end{aligned} \quad (4.14)$$

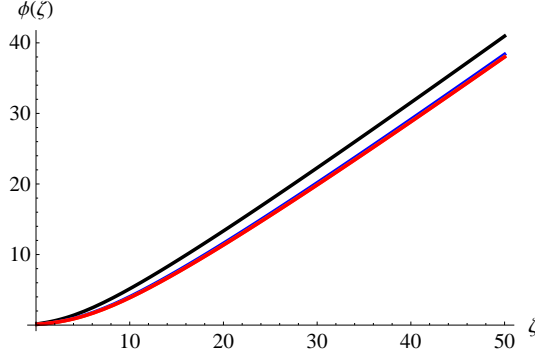


Figure 2: Solution to Eq. (4.13) for different values of $\phi'_\zeta(\zeta=0; b)$ (from top to bottom $\phi'_\zeta(\zeta=0; b) = 2$ (black), 0.2 (blue), 0 (red)).

Generally speaking we cannot satisfy Eq. (4.14) using the solution of Eq. (4.13) since these conditions depend not only on ζ but on extra variable Y . However, at large value of Y one can see that Eq. (4.14) degenerates to

$$\phi(\zeta=0; b) = \phi_0; \quad \frac{d\phi(\zeta=0; b)}{d\zeta} = 0; \quad (4.15)$$

which are consistent with the solution being the function of only ζ . In Fig. 2 we plot the numerical solution to the Eq. (4.13) at different values of $\phi'_\zeta(\zeta=0; b)$. One can see that this solution is not sensitive to this value if it is small enough. It means that the ζ scaling behaviour can start from rather small values of Y . Since the whole approach, based on leading $\log(1/x)$ contribution, can be trusted only at large values of Y we believe that ζ scaling behaviour is a good approximation to the solution of Eq. (3.8).

4.5 Numerical solution

It turns out that this believe was too optimistic. In Fig. 3 we plot the numerical solution to Eq. (3.8) with the initial condition given by Eq. (4.2). The main lesson that we can learn from these pictures is that the ζ - scaling behaviour can be reasonable approach but at unreasonably large values of l or/and Y . Indeed, at Fig. 3-b we can see that at large values of ζ the solution depends on l only slowly.

At large Y and l the exact solution is reasonable to compare with the solution of Eq. (4.13) (see Fig. 4). One can see the same pattern: they become close at large values of Y and l (ζ and l).

5. Conclusions

In this paper we show that the intuitive guess that the running QCD coupling will violate the geometric behaviour of the scattering amplitude, turns out to be correct. Indeed, we found out that the new dimensional scale: Λ_{QCD} , that brings the running α_S , enters to the amplitude behaviour even at very high energies. However, in the vicinity of the saturation scale ($r^2 \propto 1/Q_s^2$) we see the geometric scaling behaviour. This vicinity is determined by $\alpha_S(Q_s) \ln(r^2 Q_s^2) \leq 1$. In other words, the geometric scaling

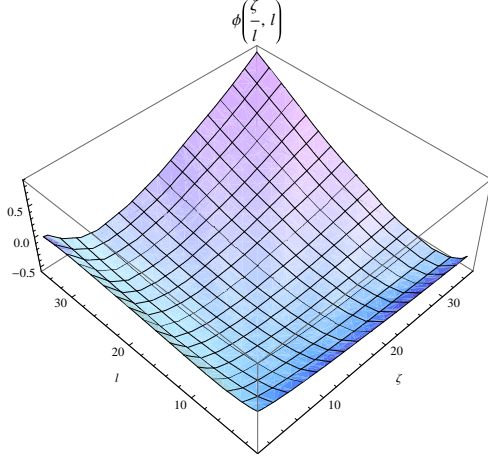


Fig. 3-a

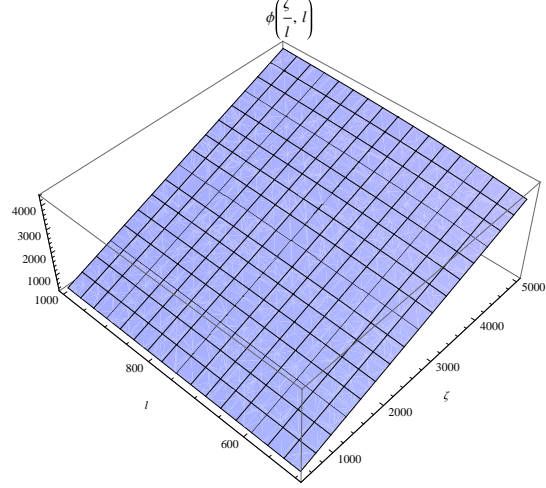


Fig. 3-b

Figure 3: The exact solution of Eq. (3.8) with the initial conditions given by Eq. (4.2) for function $\phi(\zeta/l, l)$. Fig. 3-a gives the behaviour of ϕ at small values of ζ and l while Fig. 3-b shows the same behaviour in the region of large ζ and l . The value of ϕ_0 was taken $\phi_0 = 0.1$

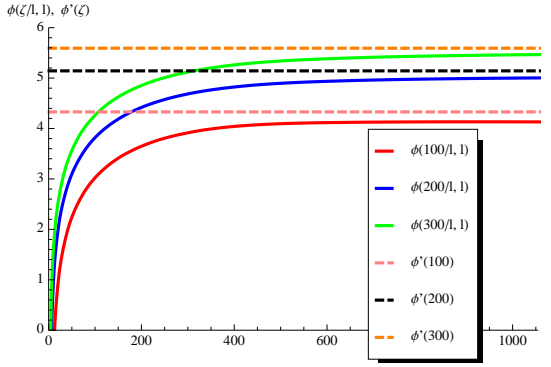


Fig. 4-a

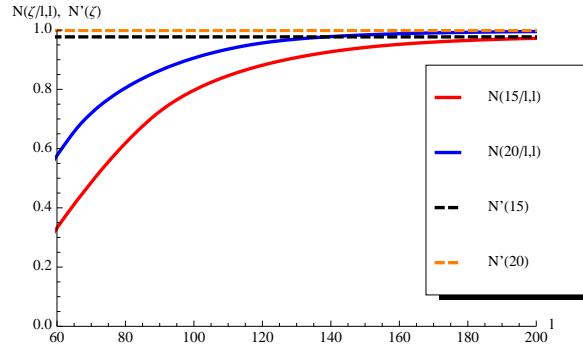


Fig. 4-b

Figure 4: The exact solution of Eq. (3.8) with the initial conditions given by Eq. (4.2) for function $\phi(Y, l)$ versus ζ -scaling solution of Eq. (4.13) $\phi'(\zeta)$. In Fig. 4-a $\ln \phi(\zeta/l, l)$ and $\ln \phi'(\zeta)$ are plotted at different values of ζ . Fig. 4-b shows the same but for the amplitude $N(\zeta/l, l) = 1 - \exp(-\phi(\zeta/l, l))$ and $N'(Y\zeta) = 1 - \exp(-\phi'(\zeta))$. The calculations were performed at $\phi_0 = 0.1$.

behaviour of the amplitude remains until we can neglect the difference between $\alpha_S(r^2)$ and $\alpha_S(1/Q_s^2)$. In different way of saying, if we could find the mechanism that will freeze the running α_S on $r^2 = 1/Q_s^2$ the amplitude would show the geometric scaling behavior. However, in the framework of the leading twist

BFKL we did not find such a mechanism.

For $\alpha_S(Q_s) \ln(r^2 Q_s^2) > 1$ the geometric scaling behaviour is violated and at very large Y and $l = \ln\left(\ln\left(r^2 \Lambda_{QCD}^2\right) / \ln\left(Q_s^2 \Lambda_{QCD}^2\right)\right)$ the amplitude depends only on one variable ζ (see Eq. (1.1)).

From our point of view the fact that we see geometric scaling behavior experimentally, stems from either we have not probed the proton at HERA and the LHC deeply inside the saturation region or that there exists the mechanism of freezing of the coupling QCD constant at $r^2 \approx 1/Q_s^2$. In practical calculations α_S is used to be frozen at some value of the momentum larger than $1/r_{fr}^2 > \Lambda_{QCD}^2$. In this case we would like to notice that if $\alpha_S(Q_s) \ln(r_{fr}^2 Q_s^2) \leq 1$ we still have the geometric scaling behaviour. For example in recent paper of Ref. [22] the value of r_{fr} is chosen from $\alpha_S(r_{fr}) = 0.7$ or 1. For such value of r_{fr} we see that $\alpha_S(Q_s) \ln(r_{fr}^2 Q_s^2) \leq 1$ for $Q_s^2 = 0.3 \div 4 \text{ GeV}^2$ covering the region of energy from RHIC to LHC. Therefore, in the CGC motivated model of Ref. [22] we do not expect to see any violation of the geometric scaling behaviour.

References

- [1] E. A. Kuraev, L. N. Lipatov, and F. S. Fadin, *Sov. Phys. JETP* **45**, 199 (1977); Ya. Ya. Balitsky and L. N. Lipatov, *Sov. J. Nucl. Phys.* **28**, 22 (1978).
- [2] L. V. Gribov, E. M. Levin and M. G. Ryskin, *Phys. Rep.* **100**, 1 (1983).
- [3] A. H. Mueller and J. Qiu, *Nucl. Phys.*, 427 **B 268** (1986) .
- [4] M. A. Braun, *Phys. Lett.* **B632** (2006) 297 [arXiv:hep-ph/0512057]; arXiv:hep-ph/0504002; *Eur. Phys. J.* **C16**, 337 (2000) [arXiv:hep-ph/0001268]; *Phys. Lett. B* **483** (2000) 115 [arXiv:hep-ph/0003004]; *Eur. Phys. J. C* **33** (2004) 113 [arXiv:hep-ph/0309293]; *Eur. Phys. J.* **C6**, 321 (1999) [arXiv:hep-ph/9706373]; M. A. Braun and G. P. Vacca, *Eur. Phys. J.* **C6**, 147 (1999) [arXiv:hep-ph/9711486].
- [5] J. Bartels, M. Braun and G. P. Vacca, *Eur. Phys. J.* **C40**, 419 (2005) [arXiv:hep-ph/0412218]; J. Bartels and C. Ewerz, *JHEP* **9909**, 026 (1999) [arXiv:hep-ph/9908454]; J. Bartels and M. Wusthoff, *Z. Phys.* **C66**, 157 (1995); A. H. Mueller and B. Patel, *Nucl. Phys.* **B425**, 471 (1994) [arXiv:hep-ph/9403256]; J. Bartels, *Z. Phys.* **C60**, 471 (1993).
- [6] L. McLerran and R. Venugopalan, *Phys. Rev. D* **49**, 2233, 3352 (1994); **D 50**, 2225 (1994); **D 53**, 458 (1996); **D 59**, 09400 (1999).
- [7] J. Jalilian-Marian, A. Kovner, A. Leonidov and H. Weigert, *Phys. Rev. D* **59**, 014014 (1999), [arXiv:hep-ph/9706377]; *Nucl. Phys.* **B504**, 415 (1997), [arXiv:hep-ph/9701284]; J. Jalilian-Marian, A. Kovner and H. Weigert, *Phys. Rev. D* **59**, 014015 (1999), [arXiv:hep-ph/9709432]; A. Kovner, J. G. Milhano and H. Weigert, *Phys. Rev. D* **62**, 114005 (2000), [arXiv:hep-ph/0004014]; E. Iancu, A. Leonidov and L. D. McLerran, *Phys. Lett.* **B510**, 133 (2001); [arXiv:hep-ph/0102009]; *Nucl. Phys.* **A692**, 583 (2001), [arXiv:hep-ph/0011241]; E. Ferreira, E. Iancu, A. Leonidov and L. McLerran, *Nucl. Phys.* **A703**, 489 (2002), [arXiv:hep-ph/0109115]; H. Weigert, *Nucl. Phys.* **A703**, 823 (2002), [arXiv:hep-ph/0004044].
- [8] I. Balitsky, [arXiv:hep-ph/9509348]; *Phys. Rev. D* **60**, 014020 (1999) [arXiv:hep-ph/9812311]
- [9] Y. V. Kovchegov, *Phys. Rev. D* **60**, 034008 (1999), [arXiv:hep-ph/9901281].

- [10] J. Bartels, E. Levin, Nucl. Phys. **B387** (1992) 617-637.
- [11] E. Levin and K. Tuchin, Nucl. Phys. **A691** (2001) 779, [arXiv:hep-ph/0012167]; **B573** (2000) 833, [arXiv:hep-ph/9908317].
- [12] S. Munier and R. B. Peschanski, Phys. Rev. D **70** (2004) 077503 [arXiv:hep-ph/0401215]; Phys. Rev. D **69** (2004) 034008 [arXiv:hep-ph/0310357]; Phys. Rev. Lett. **91** (2003) 232001 [arXiv:hep-ph/0309177].
- [13] E. Iancu, K. Itakura, L. McLerran, Nucl. Phys. **A708** (2002) 327-352. [hep-ph/0203137]
- [14] I.I.Balitsky, Phys. Rev. **D 75** (2007),014001; Y.V. Kovchegov and H. Weigert, Nucl. Phys. **A 784** (2007), **789** (2007) 260.
- [15] A. H. Mueller and D. N. Triantafyllopoulos, Nucl. Phys. **B640** (2002) 331 [arXiv:hep-ph/0205167]; D. N. Triantafyllopoulos, Nucl. Phys. **B648** (2003) 293 [arXiv:hep-ph/0209121]
- [16] V. N. Gribov and L. N. Lipatov, Sov. J. Nucl. Phys **15** (1972) 438; G. Altarelli and G. Parisi, Nucl. Phys. **B 126** (1977) 298; Yu. I. Dokshitser, Sov. Phys. JETP **46** (1977) 641.
- [17] A.H. Mueller, Nucl.Phys. **B643** (2002) 501.
- [18] E. Levin, K. Tuchin, Nucl. Phys. **A693** (2001) 787-798. [hep-ph/0101275].
- [19] A. M. Stasto, K. J. Golec-Biernat, J. Kwiecinski, Phys. Rev. Lett. **86** (2001) 596-599, [hep-ph/0007192]; L. McLerran, M. Praszalowicz, Acta Phys. Polon. **B42** (2011) 99, [arXiv:1011.3403 [hep-ph]] **B41** (2010) 1917-1926, [arXiv:1006.4293 [hep-ph]]. M. Praszalowicz, [arXiv:1104.1777 [hep-ph]], [arXiv:1101.0585 [hep-ph]].
- [20] A. Kovner and U. A. Wiedemann, Phys. Lett. B **551** (2003) 311 [arXiv:hep-ph/0207335]; Phys. Rev. D **66** (2002) 034031 [arXiv:hep-ph/0204277]; Phys. Rev. D **66** (2002) 051502 [arXiv:hep-ph/0112140]. .
- [21] Andrei D. Polyanin and Valentin F. Zaitsev, “ *Handbook of nonlinear Partial Differential Equations*”, Chapman & Hall/CRC, 2004.
- [22] J. L. Albacete, N. Armesto, J. G. Milhano, P. Q. Arias, C. A. Salgado, [arXiv:1012.4408 [hep-ph]].